SUPPLEMENTAL DATA

Table S1. CRAPome analysis of candidate DDR factors identified by PICh
List of 78 human orthologs of mouse proteins that were enriched at least 2 fold at dysfunctional telomeres in PICh on mouse telomeres with and without TRF2. Proteins are ranked based on CRAPome score (http://www.crapome.org), representing the number of times they were identified in 411 proteomics studies. Proteins identified in greater than 25% of proteomics studies (red) are considered likely contaminants. Known DNA damage response factors are highlighted in bold. PHF11 is in blue.

Table S1

NAB1	0	NAT10	70
SENP7	**0**	MSN	78
PHF11	1	LRRC59	80
TOPBP1	**4**	RPN2	82
IKBIP	8	MAP4	86
PML	9	RPN1	91
RRP9	10	NOP2	91
SEC63	11	VARS	100
POLR1B	11	SSB	102
RBM19	12	RPL28	109
EMC1	12	PLEC	109
ASPH	14	SND1	118
POLR1A	17	CANX	126
NOMO1	19	GNB2L1	135
NOL11	25	G3BP1	141
SRPR	25	RUVBL2	141
UTP18	26	RPL13A	144
ITGB1	26	SNRNP200	146
HSD17B12	27	RUVBL1	152
WDR43	27	RAN	154
SEC61A1	28	EEF1D	157
HEATR1	34	RPL3	163
BCAP31	36	MYH10	166
NOL6	36	VCP	167
PDCD11	38	RPS9	170
WDR36	41	FLNB	171
53BP1	**41**	PABPC1	172
MDC1	**42**	RPL6	172
TBL3	42	SERBP1	175
LYAR	44	EEF1G	193
MTDH	50	RPL4	197
RBM28	54	RPL7A	197
RRBP1	58	RPS16	211
CKAP4	58	RPS4X	225
RIF1	**61**	RPS18	225
HMGA1	70	RPL23	243
AHNAK	70	RPS14	259
DDX18	70	HNRNPU	280
SMARCC1	70	HNRNPK	288

Figure S1. Gong et al.

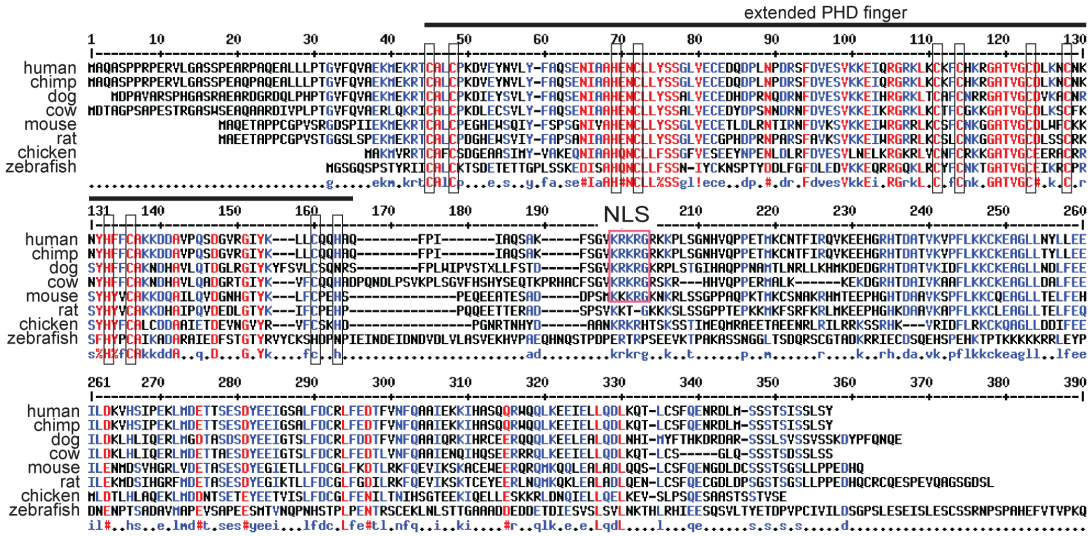

Figure S1. PHF11 orthologs in vertebrates.
Multalin (http://multalin.toulouse.inra.fr/multalin/) alignment of the PHF11 proteins from the indicated species. The zebrafish sequence is truncated at the C-terminus. The extended PHD finger and the NLS are highlighted.

Figure S2. Gong et al.

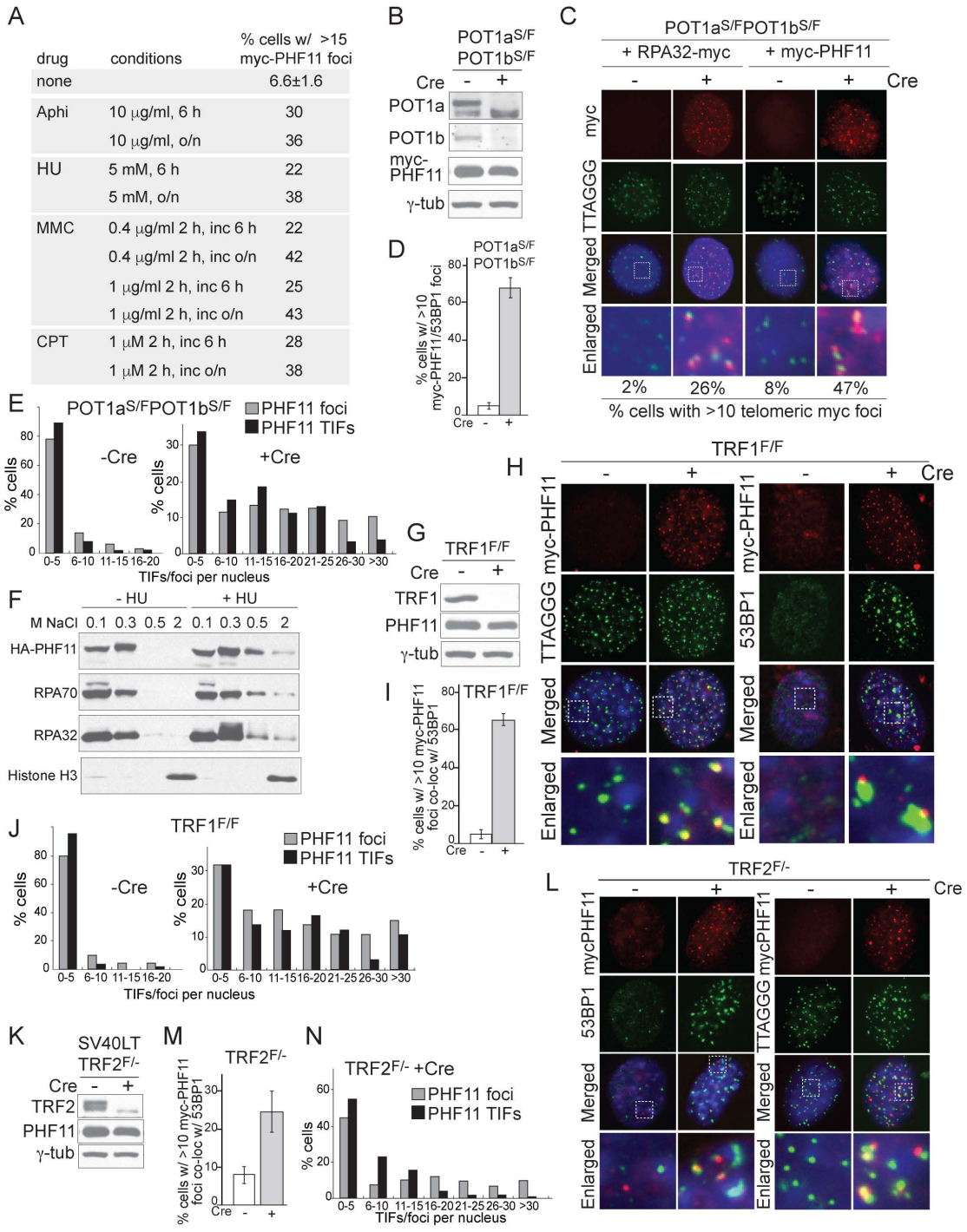

Figure S2. PHF11 focus formation at sites of DNA damage.
(*A*) PHF11 foci at sites of DNA damage induced by aphidicolin (Aphi), hydroxyurea (HU), mitomycin C (MMC), and camptothecin (CPT) treatment with the indicated regimens. (*B*) Immunoblot for deletion of POT1a and POT1b from POT1a/b DKO MEFs expressing myc-PHF11 used in Fig. 1D. (*C*) Formation of

RPA32-myc and myc-PHF11 foci at telomeres (TIFs) lacking POT1a/b. *(D)* Quantification of myc-PHF11 foci that co-localize with 53BP1 before and after deletion of POT1a/b. See legend to Fig. 1E for method. (*E*) Distribution of frequencies of myc-PHF11 foci or myc-PHF11 foci at telomeres after deletion of POT1a/b (72 h post-Cre). See legend to Fig. 1E for method. (*F*) Damage-induced chromatin binding of PHF11. MEFS were treated with 5 mM HU for 6 h (or not) and nuclear proteins were sequentially fractionated with the indicated salt concentrations. Extracted proteins were detected by immunoblotting. *(G)* Immunoblot for deletion of TRF1 from $TRF1^{F/F}$ MEFs expressing myc-PHF11. (*H*) IF and IF-FISH for myc-PHF11 foci co-localizing with 53BP1 and telomeres 72 h after deletion of TRF1 with Cre. (*I*) and (*J*) Quantification and distribution of myc-PHF11 foci in MEFs lacking TRF1. As in (*D*) and (*E*). (*K*) Immunoblot for deletion of TRF2 from SV40LT-$TRF2^{F/-}$ MEFs expressing myc-PHF11. (*L*) IF and IF-FISH for myc-PHF11 foci co-localizing with 53BP1 and telomeres at 72 h after deletion of TRF2 with Cre. (*M*) and (*N*) Quantification and distribution of myc-PHF11 foci in MEFs lacking TRF2. As in (*D*) and (*E*).

Figure S3. Gong et al.

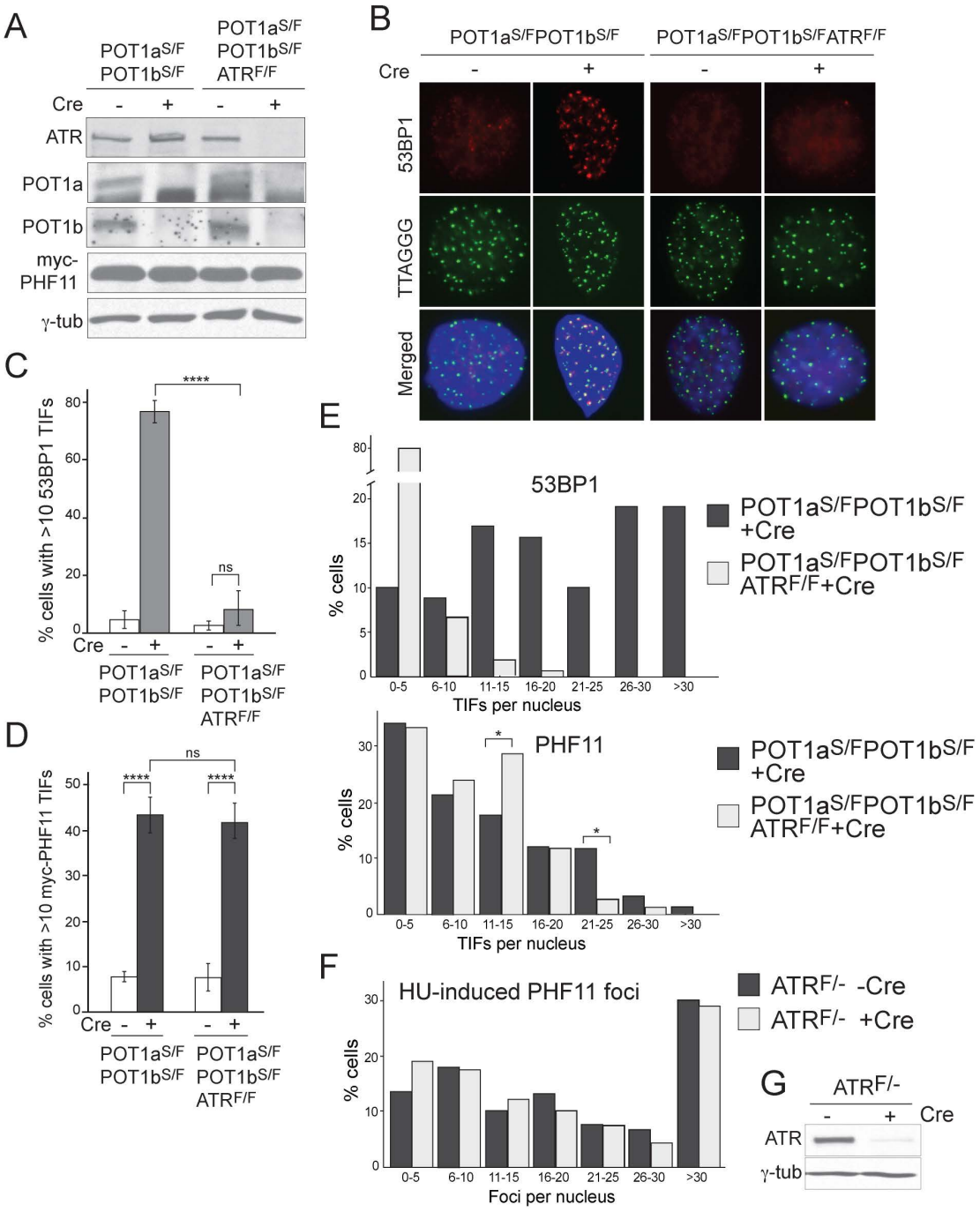

Figure S3. Effect of ATR on the accumulation of PHF11 at telomeres lacking POT1a/b.

(*A*) Immunoblot demonstrating expression of myc-PHF11, the loss of POT1a/b, and absence of ATR in the indicated cell lines treated with Cre. (*B*) IF-FISH to detect 53BP1 TIFs in POT1a/b DKO cells with and without ATR. See legend to Fig. 1D for method. (*C*) Quantification showing induction of 53BP1 foci at

telomeres after deletion of POT1a/b and the lack of 53BP1 induction when ATR is absent. Based on data as in (*B*). Averages of three independent experiments and SDs. p<0.0001 (unpaired Student t-test). (*D*) Quantification showing induction of myc-PHF11 foci at telomeres after deletion of POT1a/b and the effect of ATR co-deletion. Based on data as in Fig. 1F. Averages of three independent experiments and SDs. ****, p<0.0001 (unpaired Student t-test). (*E*) Distribution of the frequency of myc-PHF11 or 53BP1 foci at telomeres in the indicated cells. Data from three independent experiments (at least 150 nuclei for each genotype). (*F*) Distribution of the frequency of myc-PHF11 foci after 2 mM HU treatment for 4 h in MEFs before and after deletion of ATR with Cre. Data from two independent experiments (at least 100 nuclei for each genotype). (*G*) Immunoblot demonstrating the deletion of the ATR kinase in the experiment in (*F*).

Figure S4. Gong et al.

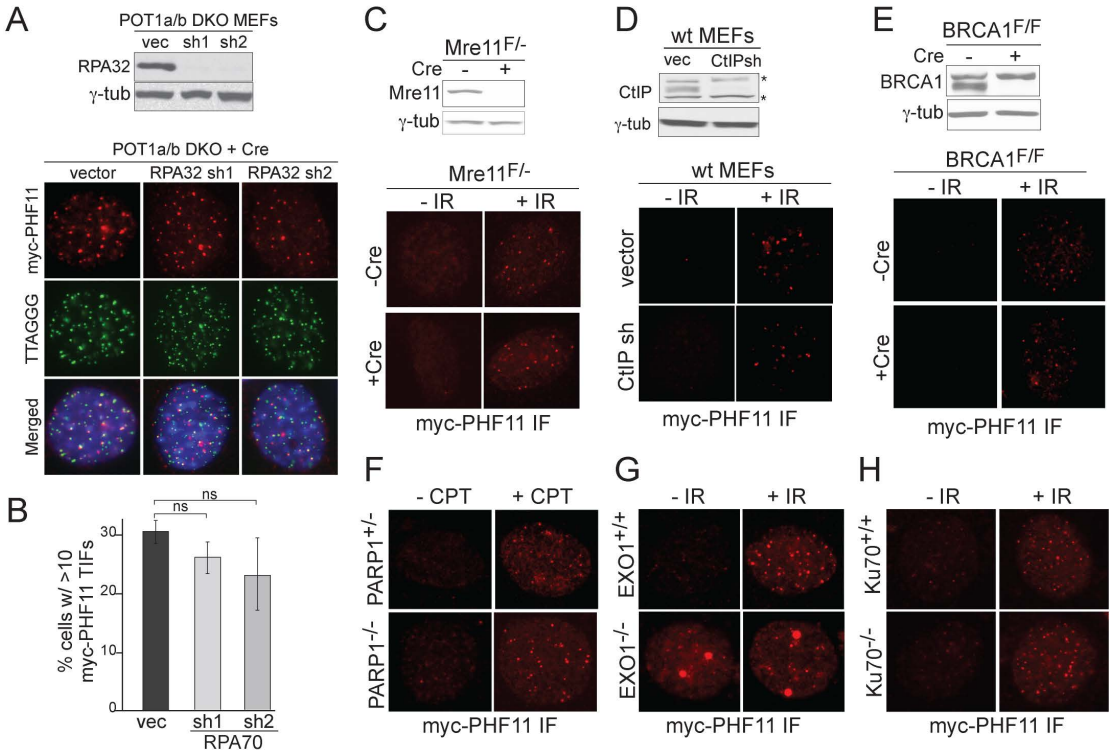

Figure S4. Effects of DDR factors on the recruitment of PHF11 to sites of DNA damage.
(*A*) Immunoblot demonstrating depletion of RPA32 using 2 shRNAs in POT1a/b DKO MEFs expressing myc-PHF11 (top). IF-FISH for myc-PHF11 TIFs at telomeres lacking POT1a/b and depleted for RPA (bottom). (*B*) Quantification of PHF11 TIFs with and without RPA shRNAs. Averages and SDs from three independent experiments. p>0.05 (unpaired Student t-test). (*C*) Immunoblot demonstrating deletion of Mre11 from $Mre11^{F/-}$ MEFs expressing myc-PHF11 (top). IF showing myc-PHF11 foci induced by 3 Gy IR (2 h) before and after deletion of Mre11 (bottom). (*D*) Immunoblot demonstrating depletion of CtIP after shRNA treatment in wt MEFs expressing myc-PHF11 (top). IF showing myc-PHF11 foci induced by 3 Gy IR (2 h) before and after CtIP shRNA (bottom). (*E*) Immunoblot demonstrating deletion of BRCA1 from $BRCA1^{F/F}$ MEFs expressing myc-PHF11 (top). IF showing myc-PHF11 foci induced by 3 Gy IR (2 h) before and after deletion of BRCA1 (bottom). (*F*) IF showing myc-PHF11 foci induced by 1 μM CPT (3 h) in $PARP1^{+/-}$ and $PARP1^{-/-}$ MEFs. (*G*) IF showing myc-PHF11 foci induced by 3 Gy IR (2 h) in $EXO1^{+/+}$ and $EXO1^{-/-}$ MEFs. (*H*) IF showing myc-PHF11 foci induced by 3 Gy IR (2 h) in $Ku70^{+/+}$ and $Ku70^{-/-}$ MEFs.

Figure S5. Gong et al.

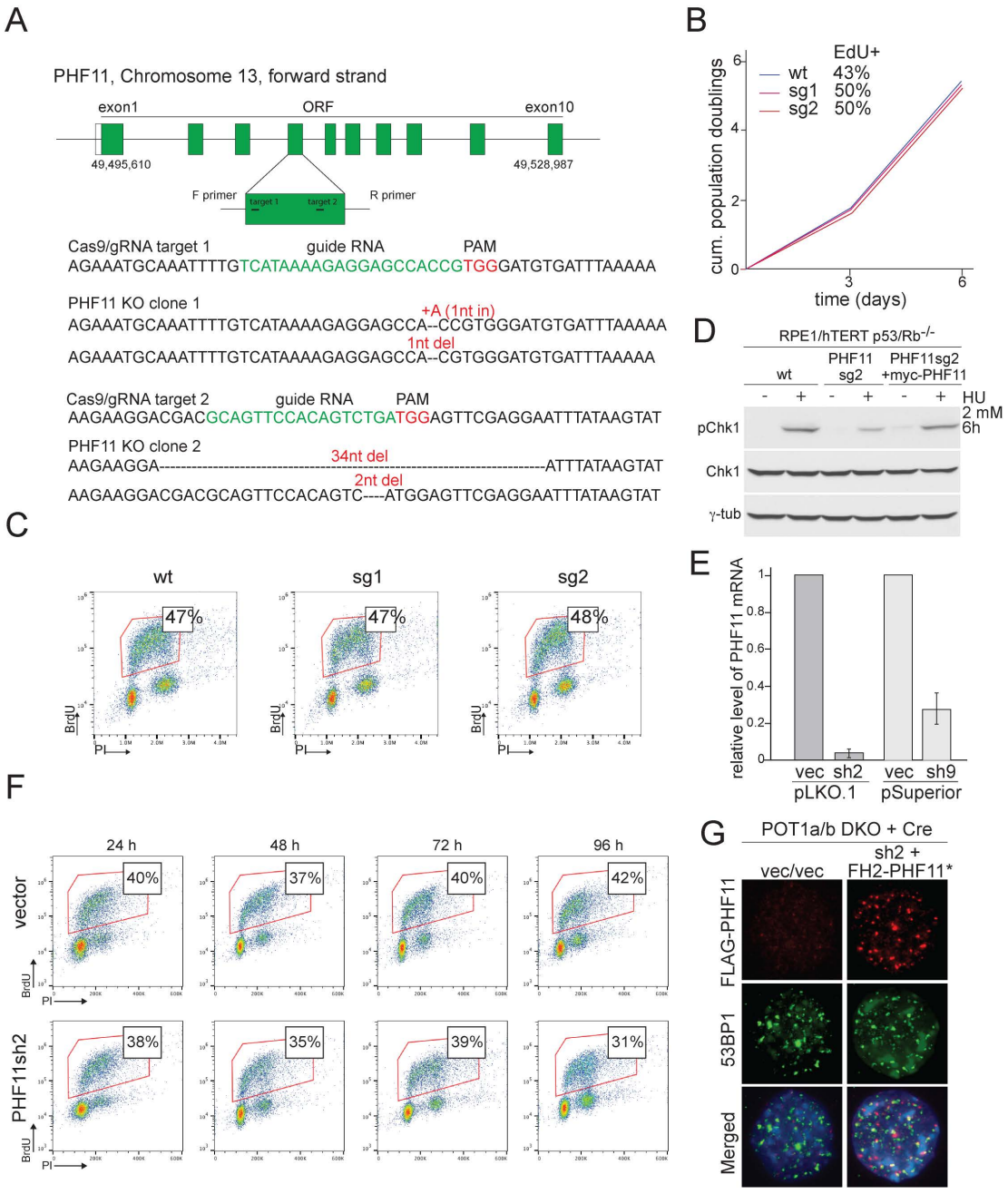

Figure S5. CRISPR/Cas9 gene-editing of PHF11 and PHF11 shRNAs. (*A*) Schematic of the PHF11 locus, the two guide RNA (gRNA) regions and their PAMs, and the sequences of the edited alleles in the two CRISPR clones used. (*B*) Growth curves of RPE1/hTERT cells lacking p53/Rb and the two PHF11 KO clones (sg1 and sg2) and their S phase indeces based on EdU incorporation. (*C*) FACS profile of wt and two PHF11 KO clones (sg1 and sg2). Cells were labelled with BrdU for 1 h. % of BrdU positive cells is indicated in each FACS profile. (*D*)

Immunoblot for Chk1 phosphorylation in wt and PHF11 KO cells with or without complementation with myc-PHF11 after HU treatment showing the functionality of myc-PHF11 and the specificity of the KO. (*E*) qRT-PCR data on the effect of the indicated PHF11 shRNAs on the abundance of PHF11 mRNA and GAPDH mRNA (control). (*F*) FACS profiles of MEFs with and without PHF11 sh2 at the indicated time points after infection to determine effects on S phase index. Cells were labelled with BrdU for 1 h. % BrdU positive cells is indicated in each FACS profile. PHF11 sh9 also has no effect on the S phase index (not shown). (*G*) shRNA-resistant PHF11 forms foci at telomeres lacking POT1a/b. IF for FH2-PHF11 (FLAG IF, red) and 53BP1 (IF, green) in POT1a/b DKO MEFs (72 h after Cre). Blue: DAPI DNA stain. 2nd panel: cells complemented with shRNA-resistant FH2-PHF11.